# APPENDIX A: LAMINAR AND TURBULENT FLAME PROPAGATION IN HYDROGEN–AIR–STEAM MIXTURES*

## A.1 Laminar Burning Velocities of Hydrogen-Air and Hydrogen-Air-Steam Mixtures

### A.1.1 Background

Methods of measuring flame velocity can be divided into 2 groups: stationary-flame and free-flame propagation methods. More detailed classification of the methods is shown in Table A.1.1-1 [A1,A.2 ] .

One of the important disadvantages of a simple tube burner is the parabolic velocity profile for unburned gas. Moreover, the apparent burning velocity varies over the defined surface (schlieren, shadow or luminous) and a mean value is obtained.

The most crucial disadvantage of the burner method is flame unsuitability in lean hydrogen-air mixtures (15% $H_2$ or less). A usual symmetrical cone is absent in such mixtures, and the flame has a polyhedral structure. It consists of several luminous reaction zones separated by dark regions. Another example of flame instability is the breakup of the flame cone top. Table A.1.1-2 summarizes the discrepancies between the burning velocity data obtained by different methods for hydrogen-air premixed flames at atmospheric pressure and room temperature [A.1,A.2]. Laminar burning velocity data for hydrogen-air mixtures are shown in Figure A.1.1-1. The nozzle burner data of Liu and MacFarlane [A.3] differ markedly from both the spherical bomb data and the Bunsen burner data. Such results may be reasonably explained by the influence of flame stretch. Liu and MacFarlane [A.3] used a very small nozzle (3 mm), and this is why they obtained a higher value for burning velocity.

The burning velocity, $S_u$ , can be calculated from the measured flame speed $S_b = dr_f /dt$ by employing the following equation:

$$S_u = S_b / \sigma \quad , \tag{A.1}$$

where $\sigma$ is the expansion ratio for constant pressure burning. This value may be determined by thermodynamic computations of the adiabatic burning temperature $T_b$ with regard to a change of the gas density in combustion:

$$\sigma = \rho_0 / \rho_b = (n_b T_b) / (n_0 T_0) \quad . \tag{A.2}$$

Here, $r_0$ and $r_b$ are the density of unburned and burned gas, $T_0$ is the initial temperature of the gaseous mixture, and $n_0$ and $n_b$ are the moles of unburned and burned gases respectively.

The values of adiabatic flame temperatures and moles of burned gases can be calculated by using available thermodynamic data JANAF. Adiabatic flame temperature $T_b$ and expansion ratio $s$ for hydrogen-air-steam mixture (f = 0.39) are shown in Table A.1.1-3.

---

*Professor Boris E. Gelfand is the lead author of Appendix A.

| $T_0$(K) | $T_b$(K) | | | s | | |
|---|---|---|---|---|---|---|
| | 0% $H_2O$ | 10% $H_2O$ | 20% $H_2O$ | 0% $H_2O$ | 10% $H_2O$ | 20% $H_2O$ |
| 293 | 1393 | - | - | 4.42 | - | - |
| 323 | 1418 | 1293 | 1175 | 4.08 | 3.75 | 3.43 |
| 373 | 1459 | 1335 | 1217 | 3.64 | 3.35 | 3.08 |
| 393 | 1476 | 1352 | 1234 | 3.49 | 3.22 | 2.96 |
| 423 | 1501 | 1378 | 1259 | 3.30 | 3.05 | 2.81 |
| 473 | 1544 | 1420 | 1302 | 3.04 | 2.81 | 2.60 |
| 523 | 1586 | 1463 | 1345 | 2.82 | 2.62 | 2.43 |

If the initial pressure $p_0$ varies from 1 to 10 bar, $T_b$ and $s$ remain practically unchanged. This is due to the insignificant dissociation of combustion products at given temperatures of lean hydrogen-air-steam mixtures. Examples of radius-flame registrations and photographs of hydrogen-air-steam flames will be shown below along with experimental data.

### A.1.2 Results of Laminar Burning Velocity Measurements in Lean $H_2$-Air and $H_2$-Air-Steam Mixtures at Room and at Elevated Temperatures

The influence of initial pressure is illustrated in Figure A.1.2-1. Solid lines correspond to our numerical predictions. Solid circles and triangles denote pressure-time and flame radius-time methods of burning velocity measurements. Experimental data obtained by Andrews and Bradley [A.4] and by Shebeko et al. [A.5] are also shown. Andrews and Bradley [A.4] used double-kernel and single-kernel methods with schlieren photography; Shebeko et al. [A.5] used p-t procedure without photography. It is interesting to note that the relative deviation of experimental and theoretical data is greater for 10% $H_2$-air mixture than for 20% $H_2$-air mixture. Moreover, the deviation increases with pressure. Numerical simulation predicts the negative pressure exponent for 10% $H_2$-air mixture, but p-t measurements do not corroborate this relationship.

### A.1.3 Temperature and Pressure Influence on Burning Velocity

Burning velocities, measured by the flame radius-time method, are shown in Figure A.1.3-1. The measurements was performed for hydrogen-air-steam mixtures at two initial pressures of 3 and 5 bar. Experimental results are in good agreement with theoretical results. This fact has substantially facilitated the solution of the pressure exponent determination problem.

#### A.1.3.1 *Pressure and temperature exponents*

A power law dependence of the following form

$$S_u = S_{u0} (T/T_0)^a (P/P_0)^b \tag{A.3}$$

is often used for burning velocity approximation. *a* is referred to as temperature exponent (or temperature index) and *b* as pressure exponent (or pressure index). $T_0$ and $P_0$ are initial values of pressure and temperature, $S_{u0} = S_u$ at $T = T_0$ and $P = P_0$.

Measured and predicted burning velocities of hydrogen-air mixtures in the range 0.5 to 10 bar at room temperature are shown in Figure A.1.2-1. The data indicate that the values of pressure exponent are negative for hydrogen-air mixtures with a hydrogen percentage of less than 15% by volume. In a similar manner, pressure exponents *b* for hydrogen-air-steam mixtures (f = 0.39) are also negative. However, the value of *b* depends upon steam concentration and initial pressure. Figure A.1.3-2 shows the influence of pressure on laminar burning velocity for hydrogen-air-steam mixtures ($\phi = 0.39$) at 393 K. As is evident from the graph, burning velocity decreases gradually with a rise of pressure. To illustrate the rate of change of the burning velocity with pressure, we plotted the relative burning velocity $S_u / S_{u0}$ as a function of initial pressure, where percent of steam was a parameter. Pressure exponents were calculated in the range of interest (3 to 5 bar) . The values of pressure exponents are indicated near the curves.

The influence of temperature on the burning velocity is illustrated in Figure A.1.3-3 (a, b, c). In Figure A.1.3-3a, we have plotted the dependence of $S_u$ on initial pressure for $H_2$-air mixture ($\phi = 0.26$) at 298 K, 373 K, and 473 K. Experimental data are in good agreement with the results of the calculations. In Figure A.1.3-3b, burning velocities are plotted as a function of initial temperature at two pressures, 1 and 4 bar. Burning velocity is seen to increase with temperature. Temperature exponent *a* is shown as a function of hydrogen concentration in the range from 10% $H_2$ to 70% $H_2$ . Temperature exponent is equal to 1.6 at 42% $H_2$ and it rises significantly at 10% $H_2$, where it is equal to 3.2. The data on the influence of steam concentration on laminar burning velocity of hydrogen–air-steam mixtures are given in Reference [A.6].

### A.1.4 Turbulent Combustion Rates in Hydrogen-Air and Hydrogen-Air-Steam Mixtures

Essential experimental results of References [A.1, A.2, A.7] are presented below. Figure A.1.4-1 shows the measured turbulent combustion rates $S_T$ of a lean hydrogen-air mixture ($\phi = 0.26$) as a function of the turbulent intensity in the pressure range from 1 to 5 bar. For comparison, laminar burning velocity $S_u$ for the mixture is about 17 cm/s at 1 bar and 8 cm/s at 5 bar. As it seen from Figure A.1.4-1, in the case of turbulent combustion, the pressure dependence is absent.

Turbulent consumption rates $S_T$ measured for hydrogen-air-steam mixtures are shown in Figures A.1.4-2 and A.1.4-3. Three hydrogen-air compositions were chosen—namely, 8% $H_2$, 10% $H_2$ and 14% $H_2$—and were diluted with steam as shown in the legends of the figures. The limiting steam concentrations and limiting turbulence intensity were found for elevated temperatures in the range 393 to 400 K at atmospheric pressure. The influence of initial pressure was investigated by comparison of experimental data at 1 bar and 3 bar, as shown in Figure A.1.4-3. An extinction regime was observed in turbulent flames of hydrogen-air-steam near-limit mixtures. Turbulent flame covers a small part of the experimental vessel. Pressure rise does not exceed 0.1 to 0.15 bar. Three examples of pressure-time curves at an extinction limit in the case of 10% steam dilution are shown in Figure A.1.4-4.

### A.1.5 Flammability Limits for Lean Hydrogen–Air–Steam Mixtures

The flammable range of $H_2$-air-steam mixtures is illustrated in Figure A.1.5-1a. Shown here are the experimental results both for upward and downward (only Kumar's data [A.8]) flame propagation. Results of measurements of limit hydrogen concentrations for the most-lean composition are slightly different, whereas considerable distinctions are observed in the region of the "nose" of the flammability curve. Most likely, the discrepancy between experimental findings involves the use of various energy deposits of ignition sources. For ignition source, energy is equal 1 to 2 J [A.1,A.2] and 40 J (Kumar), and the measurements are in a good agreement. According to Figure A.1.5-1a, turbulent extinction limits lie between upward and downward laminar combustion limits.

The influence of initial temperature $T_0$ [A.1-A.3] and steam dilution on the limit hydrogen concentrations $(H_2)_{lim}$ at different fixed initial pressure is given in Figure A.1.5-1 (b, c), respectively. With a rise of $T_0$, $(H_2)_{lim}$ decreases, approximately, on the value 0.45% (vol) for every 100 K, and this value practically does not change up to 7 bar. With steam dilution up to 50% (vol), $(H_2)_{lim}$ increases on the value 0.34% (vol) for every 10% $H_2O$ (vol) at initial pressures of 1 bar and 7 bar.

The effect of the extent to which the residence time (of up to 2 h)—i.e., time interval between the moment of acquiring the desirable temperature by the hydrogen–air mixture and initiation of spark ignition—and, consequently, the existence of pre-ignition reactions that may influence the value of the flammability limits was investigated [A.3]. In the temperature range up to 473 K, the limits were not affected by the length of the residence time. However at T > 473 K, the flammability limits—especially the rich limit—narrowed with an increase in the temperature and were very significantly affected by the length of the residence time before spark ignition. This means that the time of exposure of the mixture to elevated temperature before initiation of ignition should be taken into consideration and should be reported together with obtained values of the limits. It was suggested [A.13] that the drop in the value of the rich limit and increase in the value of the lean limit with the increase of the residence time were caused by relatively low-temperature catalytic reactions on the stainless steel surface of the test tube.

## A.2 References

[A.1] Laminar and Turbulent Flame Propagation in $H_2$ + Air + Steam Mixtures at Accident Relevant Pressure at Temperature Conditions, IChPh RAS at INR FZK Research Report, 1995.

[A.2] Laminar and Turbulent Flame Propagation in $H_2$ + Air + $CO_2$ Mixtures at Accident Relevant Pressure at Temperature Conditions, IChPh RAS at INR FZK Research Report, 1996.

[A.3] D. Liu and R. MacFarlane, Laminar Burning Velocities of $H_2$ – Air and $H_2$ –Air –Steam Flames, Combustion and Flame, Vol. 49, 1983, 59-71.

[A.4 ] G. Andrews and D. Bradley, Determination of Burning Velocities : A Critical Review.
Comb. Flame Limits of $H_2$ – $O_2$- Diluent Mixtures, Journal of Fire Sciences, Vol. 3, 1985, 242-262.

[A.5] Shebeko et al.

[A.6] B.W. Marshall, Hydrogen–Air–Steam Flammability Limits and Combustion Characteristics in the FITS Vessel, NUREG Report, CR –3468, 1986.

[A.7] S. Heimel, Effect of Initial Mixture Temperature on Burning Velocity of Hydrogen-Air Mixtures with Preheating and Simulated Preburning, NASA TN- 3833, 1956.

[A.8] T. Iijima and T. Takeno, Effects of Temperature and Pressure on Burning Velocity, Combustion and Flame, Vol. 65, 1986, 35-43.

[A.9] C.K. Wu and C.K. Low, On the Determination of Laminar Flame Speeds from Stretched Flames, Proc. of 20th Symp. ( International ) on Combustion, Combustion Institute, Pittsburgh, 1984, 1941-1949.

[A.10] I . Wierzba and B.B. Ale, Effects of Temperature and Time of Exposure on the Flammability Limits of Hydrogen–Air Mixtures, International Journal of Hydrogen Energy, Vol. 23, 1998, 1197.

[A.11] D.R . Dowdy, D.B. Smith and S.C. Taylor, The Use of Expanding Spherical Flames to Determine Burning Velocities and Stretch Effects in Hydrogen–Air Mixtures, Proc. of 23rd Symp. ( International) on Combustion, Combustion Institute, Pittsburgh, 1990, 325- 331.

[A.12] M. Berman and J.C. Cummings, Hydrogen Behavior in Light–Water Reactors, Nuclear Safety, Vol. 25, 1984, 61-70.

[A.13 ] G.W. Koroll and S.R . Mulpuru, The Effect of Dilution with Steam on The Burning Velocity and Structure of Premixed Hydrogen Flames, Proc. of 21st Symp. (International) on Combustion, Combustion Institute, Pittsburgh, 1986, 1811-1819.

**Table A.1.1-1 Experimental methods for burning velocities determination**

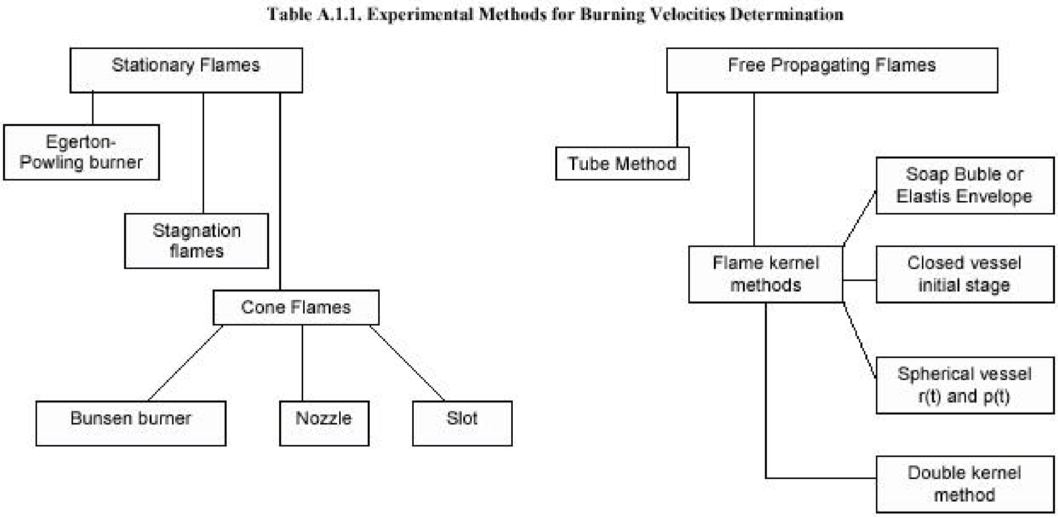

**Table A.1.1-2 Hydrogen-air laminar burning velocities (cm/s) at atmospheric pressure and room temperature**

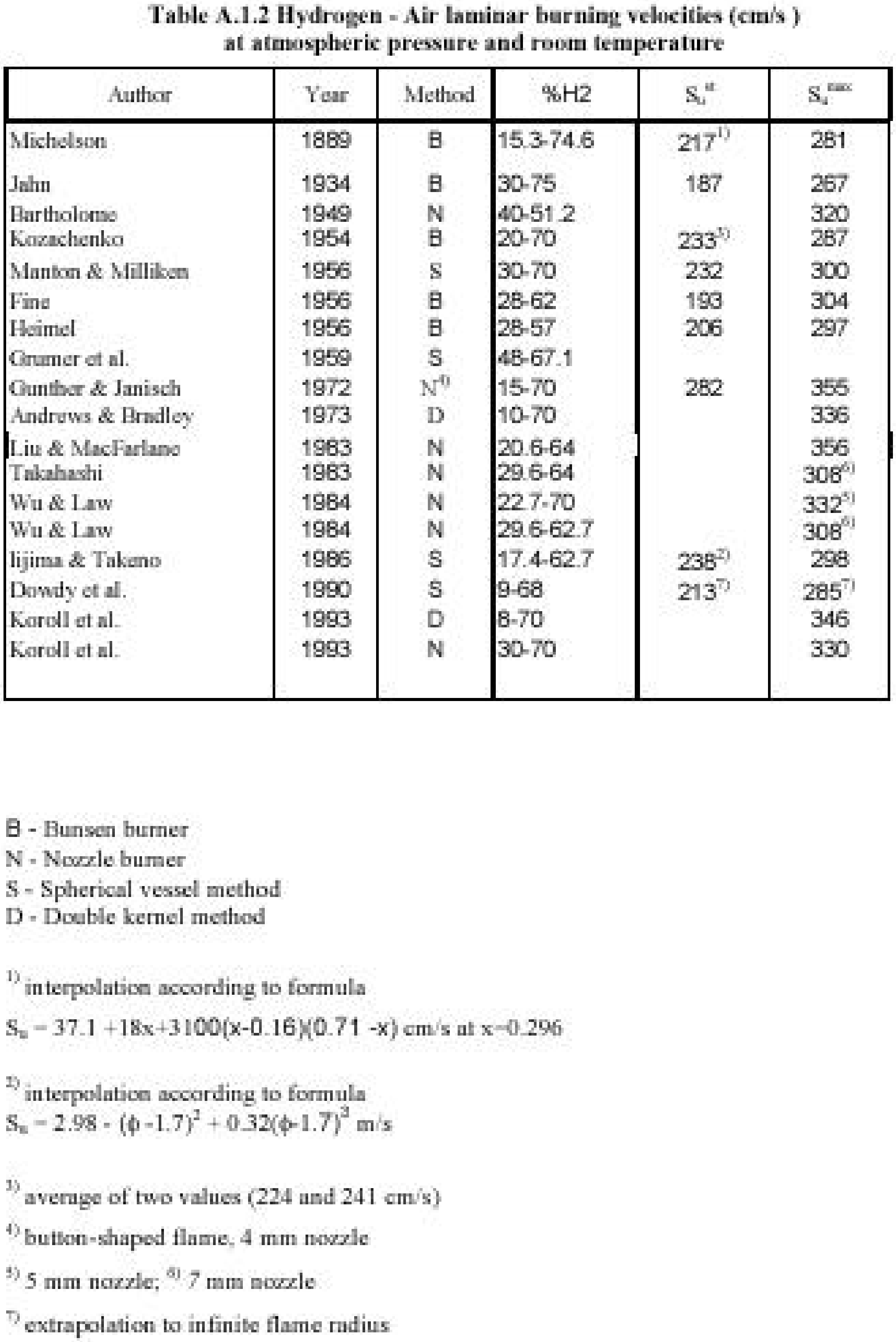

**Table A.1.2 Hydrogen - Air laminar burning velocities (cm/s ) at atmospheric pressure and room temperature**

| Author | Year | Method | %H2 | $S_u^{st}$ | $S_u^{max}$ |
|---|---|---|---|---|---|
| Michelson | 1889 | B | 15.3-74.6 | 217[1] | 281 |
| Jahn | 1934 | B | 30-75 | 187 | 267 |
| Bartholome | 1949 | N | 40-51.2 | | 320 |
| Kozachenko | 1954 | B | 20-70 | 233[3] | 287 |
| Manton & Milliken | 1956 | S | 30-70 | 232 | 300 |
| Fine | 1956 | B | 28-62 | 193 | 304 |
| Heimel | 1956 | B | 28-57 | 206 | 297 |
| Grumer et al. | 1959 | S | 48-67.1 | | |
| Gunther & Janisch | 1972 | N[4] | 15-70 | 282 | 355 |
| Andrews & Bradley | 1973 | D | 10-70 | | 336 |
| Liu & MacFarlane | 1983 | N | 20.6-64 | | 356 |
| Takahashi | 1983 | N | 29.6-64 | | 308[6] |
| Wu & Law | 1984 | N | 22.7-70 | | 332[5] |
| Wu & Law | 1984 | N | 29.6-62.7 | | 308[6] |
| Iijima & Takeno | 1986 | S | 17.4-62.7 | 238[2] | 298 |
| Dowdy et al. | 1990 | S | 9-68 | 213[7] | 285[7] |
| Koroll et al. | 1993 | D | 8-70 | | 346 |
| Koroll et al. | 1993 | N | 30-70 | | 330 |

B - Bunsen burner
N - Nozzle burner
S - Spherical vessel method
D - Double kernel method

[1] interpolation according to formula

$S_u = 37.1 + 18x + 3100(x-0.16)(0.71-x)$ cm/s at $x = 0.296$

[2] interpolation according to formula
$S_u = 2.98 - (\phi - 1.7)^2 + 0.32(\phi - 1.7)^3$ m/s

[3] average of two values (224 and 241 cm/s)

[4] button-shaped flame, 4 mm nozzle

[5] 5 mm nozzle; [6] 7 mm nozzle

[7] extrapolation to infinite flame radius

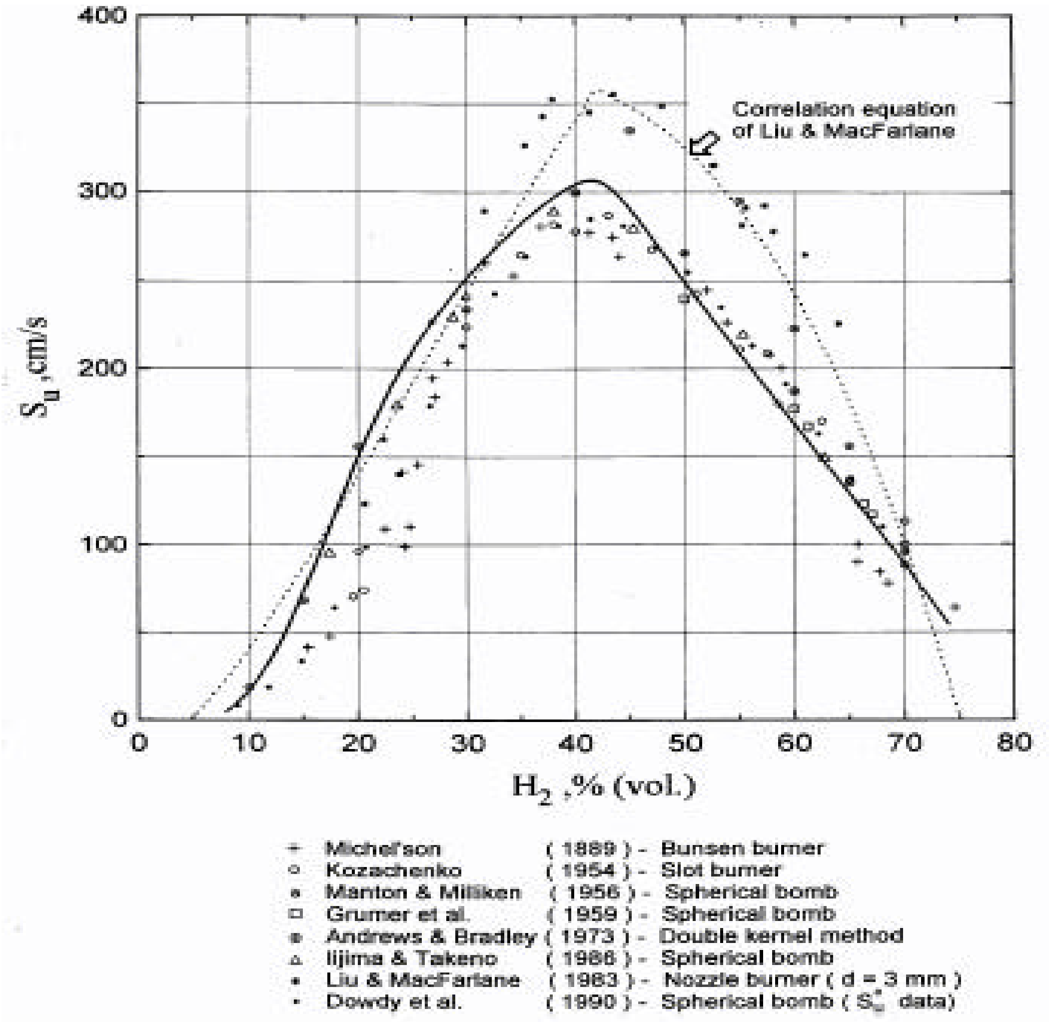

Figure A.1.1. Laminar burning velocity of hydrogen/air mixtures at room temperature and atmospheric pressure measured by various methods. Solid line: computed values for spherical flame propagation; dotted line: correlation equation of Liu and MacFarlane.

**Figure A.1.1-1 Laminar burning velocity of hydrogen air mixtures at room temperature and atmoshpheric measured by various methods. Solid line computed values for spherical flame propagation; dotted line correlation equation of Liu and MacFarlane.**

**Figure A.1.2-1 Dependence of the laminar burning velocity $S_T$ on initial pressure $P_0$ for lean hydrogen-air mixtures at 298 K. Solid lines: calculations; points: experimental data.**

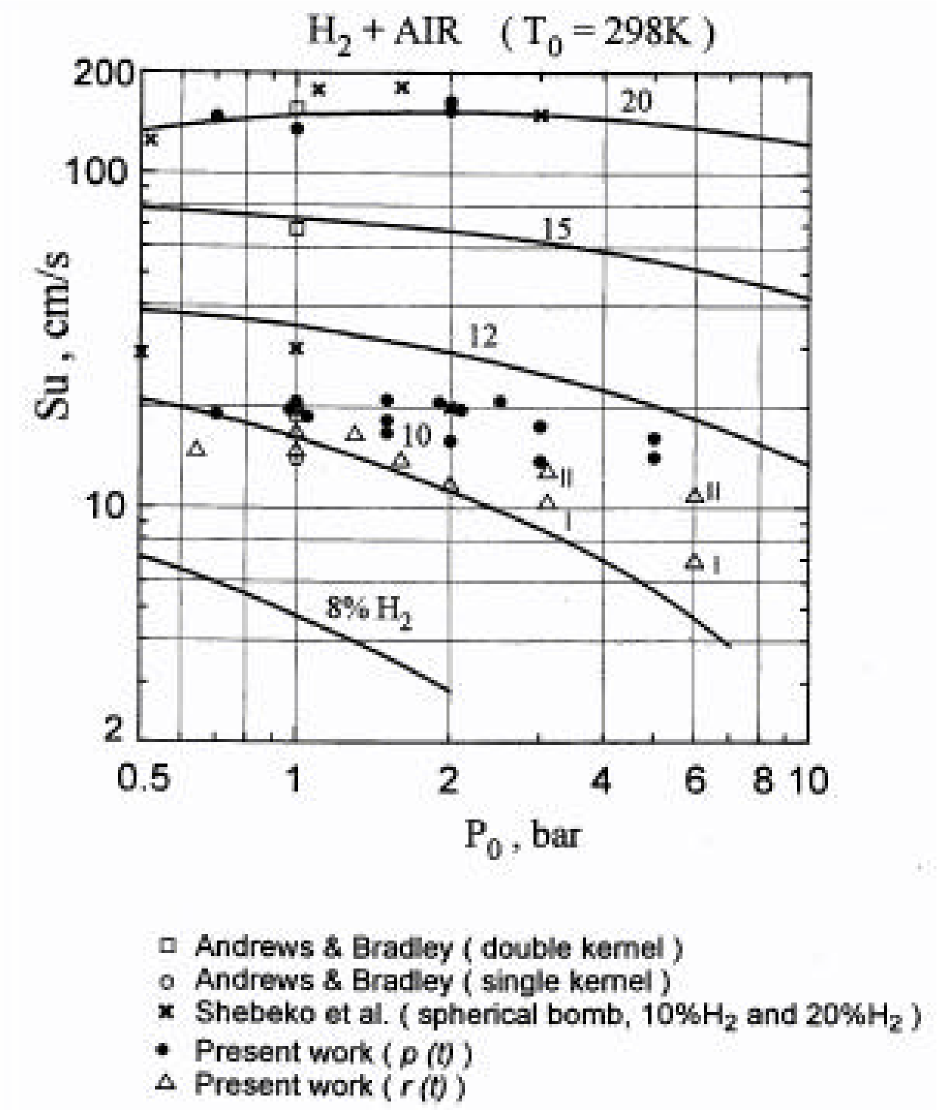

Figure A.1.2. Dependence of the laminar burning velocity $S_u$ on initial pressure $P_0$ for lean hydrogen/air mixtures at 298K. Solid lines: calculations; points: experimental data.

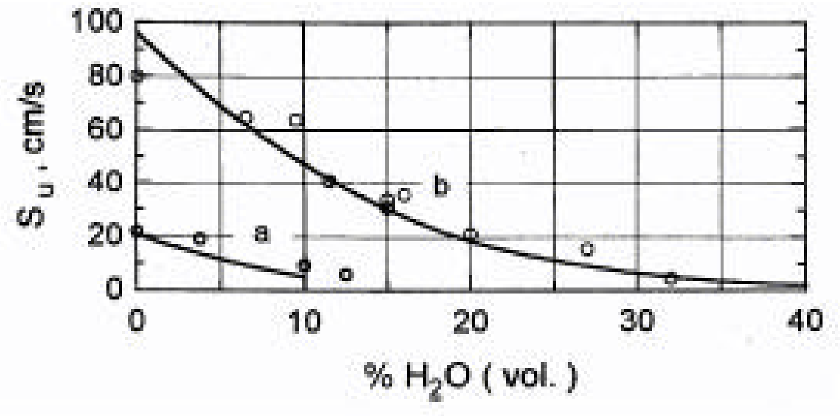

Figure A.1.3. Comparison between measured (points) and calculated (solid lines) laminar burning velocities for hydrogen-air-steam mixtures.

(a) –$T_0$=393K, $P_0$=5bar, $\phi$=0.26; (b) –$T_0$=393K, $P_0$=3bar, $\phi$=0.39

**Figure A.1.3-1 Comparison between measured (points) and calculated (solid lines) laminar burning velocities for hydrogen-air-steam mixutes.**

**(a) -$T_0$ = 393 K, $P_0$ = 5 bar, f = 0.26; (b) -$T_0$ = 393 K, $P_0$ = 3 bar, f = 0.39**

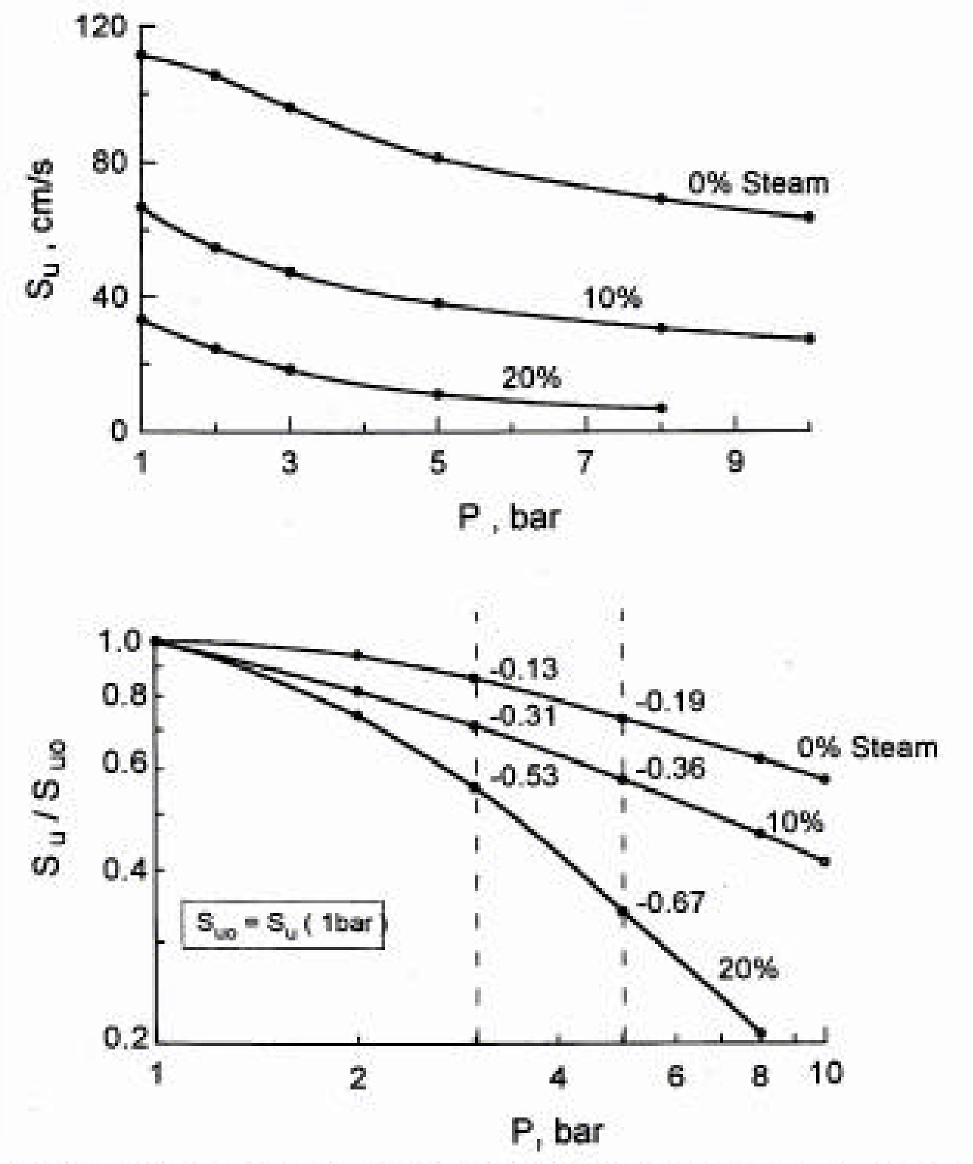

Figure A.1.4. Effect of pressure on the laminar burning velocity of hydrogen-air-steam mixtures (ϕ=0.39) at 393K. Numbers on curves indicate pressure exponent.

**Figure A.1.3-2 Effect of pressure on the laminar burning velocity of hydrogen-air-steam mixtures ( f = 0.39) at 393 K. Numbers on curves indicate pressure exponent.**

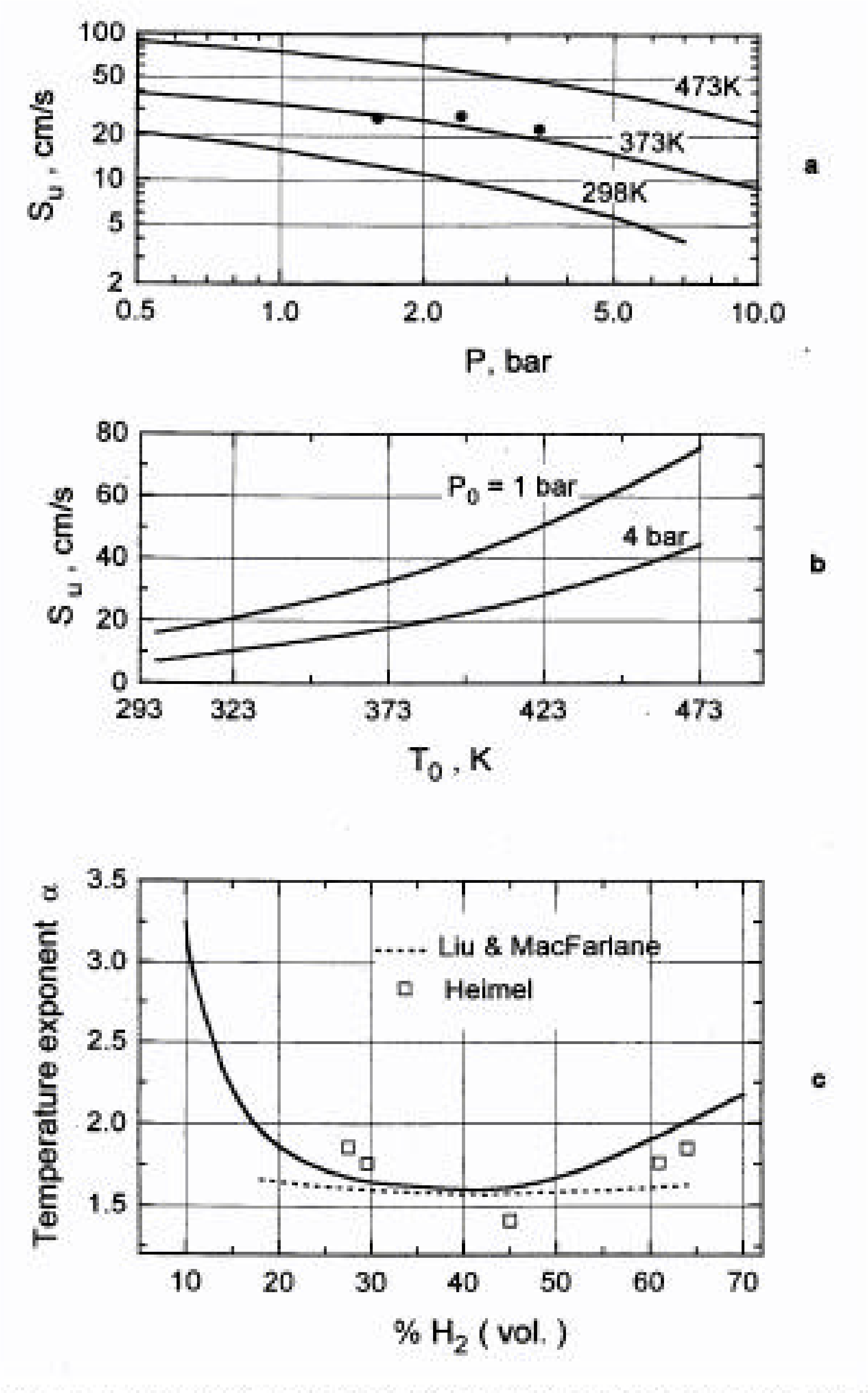

Figure A.1.5. Laminar burning velocity as a function of pressure (a) and temperature (b) for 10% $H_2$ - air mixture ($\phi$ = 0.26). (c) - Comparison between theoretical and experimental data for temperature exponent α in $H_2$ - air mixtures at 29% and 1 bar.

**Figure A.1.3-3 Laminar burning velocity as a function of pressure (a) and temperature (b) for 10% $H_2$-air mixture (f = 0.26. ( c) Comparison between theoreticla and experimental data for temperature exponent a in $H_2$-air mixtures at 29% and 1 bar.**

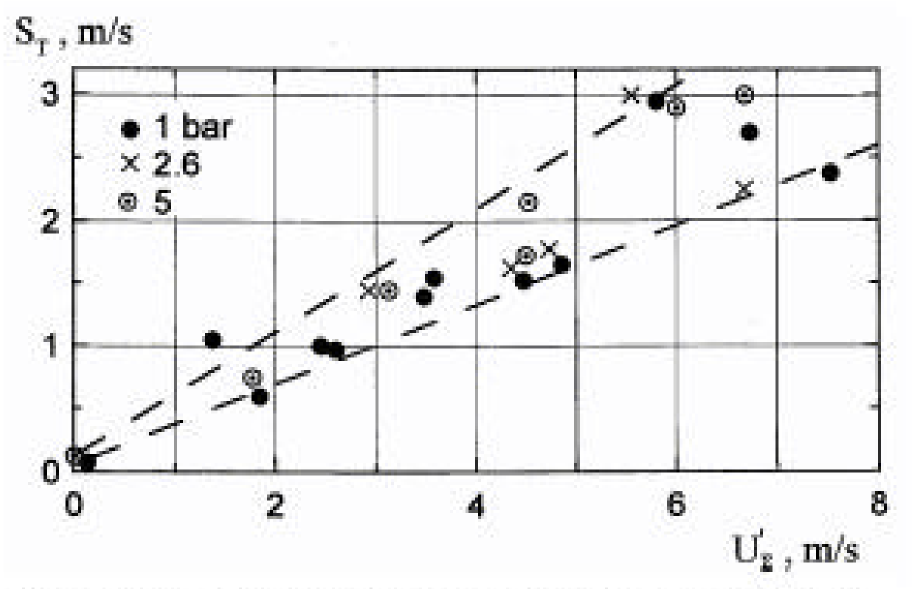

Figure A.1.6. Turbulent. consumption rate $S_T$ for $H_2$- air mixture ($\phi$ = 0.26) at 298K.

**Figure A.1.4-1 Turbulent consumption rate $S_T$ for $H_2$ -air mixture (f = 0.26) at 298 K.**

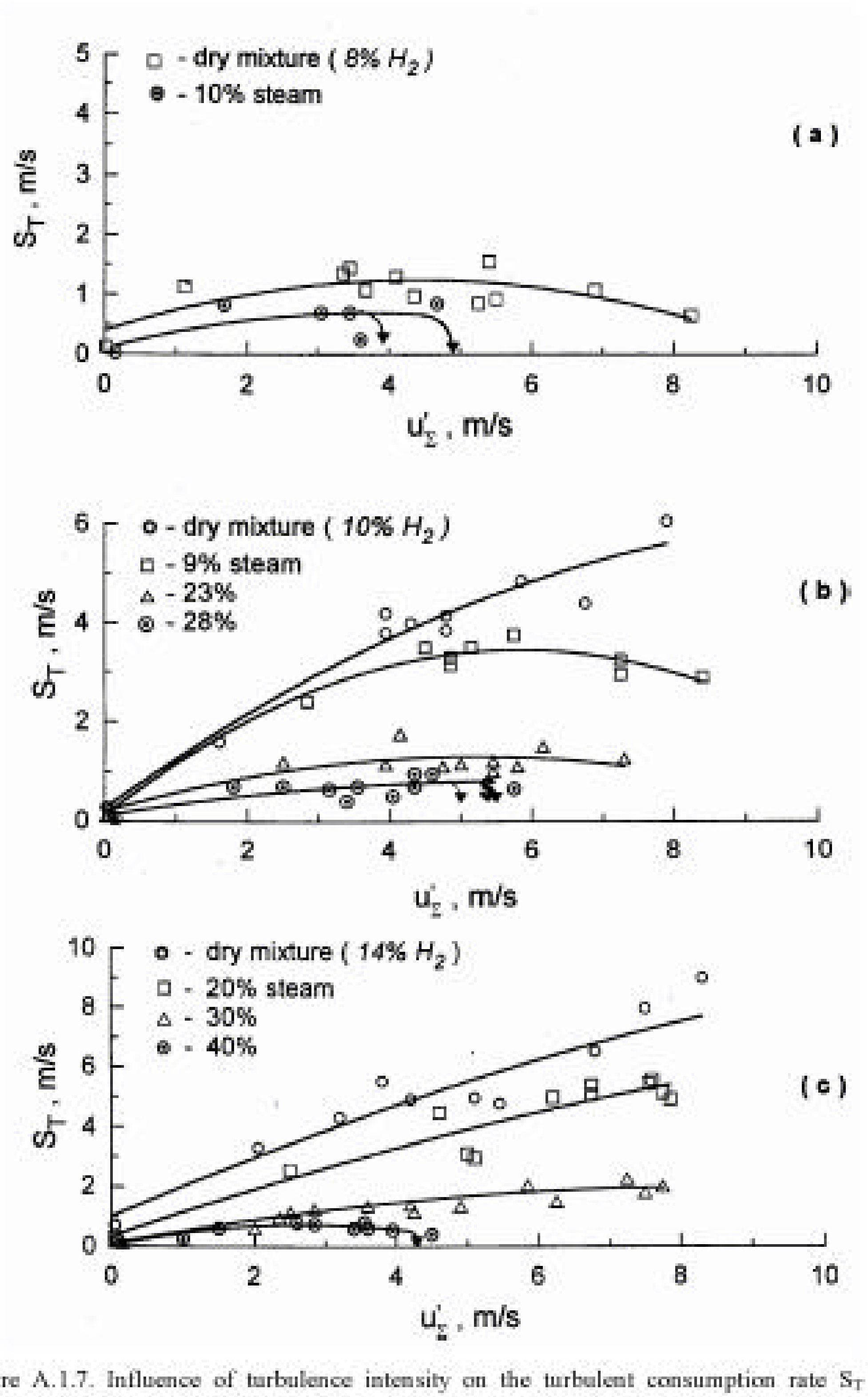

Figure A.1.7. Influence of turbulence intensity on the turbulent consumption rate $S_T$ for hydrogen-air-steam mixtures at temperatures 393 - 400K and atmospheric pressure a) φ = 0.207; b) φ = 0.26; c) φ = 0.39.

**Figure A.1.4-2 Influence of turbulence intensity on the turbulent consumption ratio $S_T$ for hydrogen-air-steam mixtures at temperatures 398 - 400 K and atmospheric pressure a) f = 0.207; b) f = 0.26; c) f = 0.39.**

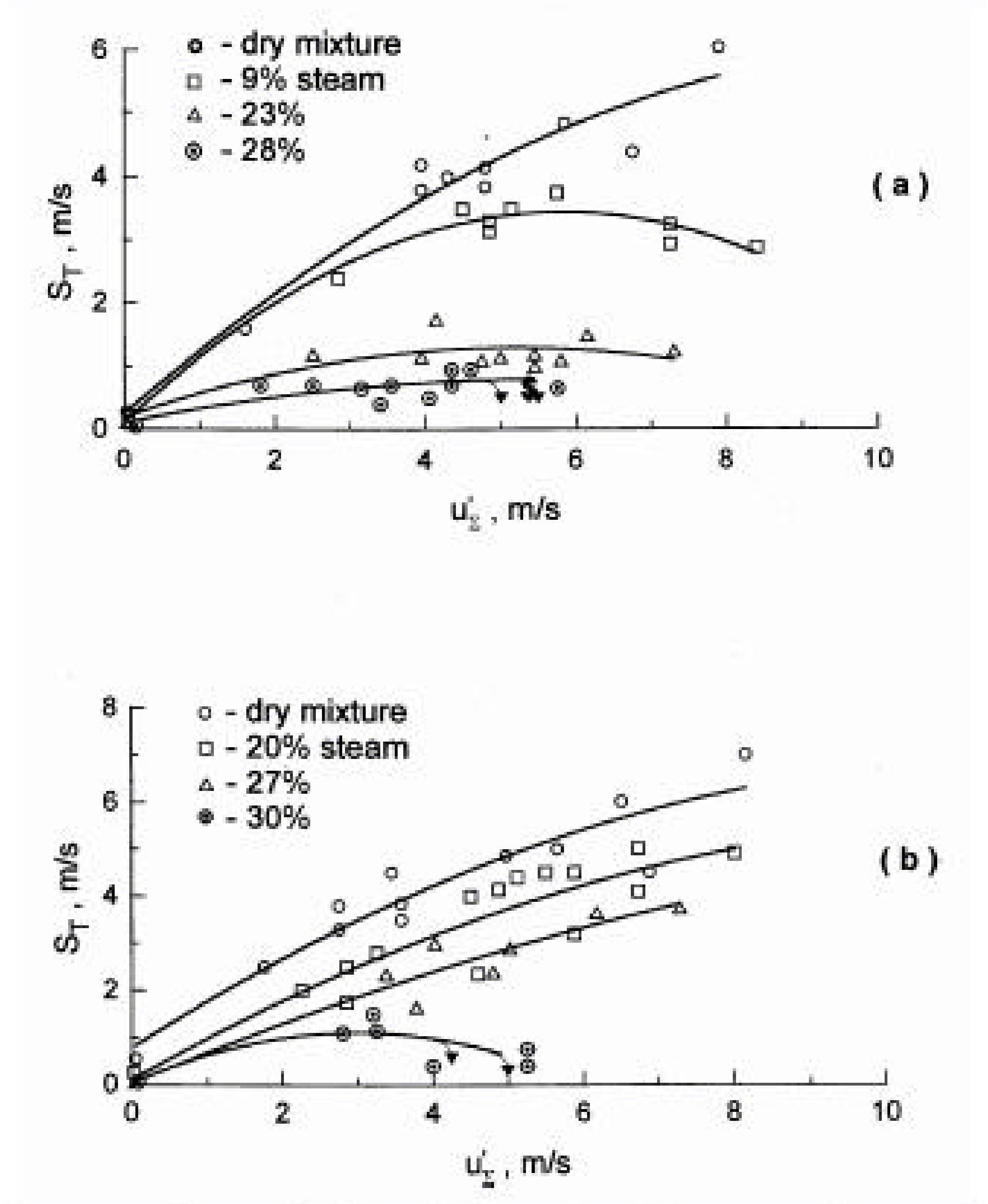

Figure A.1.8. Influence of turbulence intensity on the turbulent consumption rate $S_T$ for hydrogen-air-steam mixtures ( $\phi = 0.26$ ) at temperatures 393 - 400K. a) $P_0$=1 bar; b)$P_0$=3 bar.

**Figure A.1.4-3 Influence of turbulence intensity on the turbulent consumption rate $S_T$ for hydrogen-air-steam mixutes (f = 0.26) at temperatures 393 - 400 K. a) $P_0$ = 1 bar; b) $P_0$ = 3 bar.**

**Figure A.1.4-4 Pressure-time curves at an extinction limit for turbulent flames in hydrogen-air-steam mixtures (f = 0.2; 10% $H_2O$; $P_0$ = l bar; $T_0$ = 398 K).**

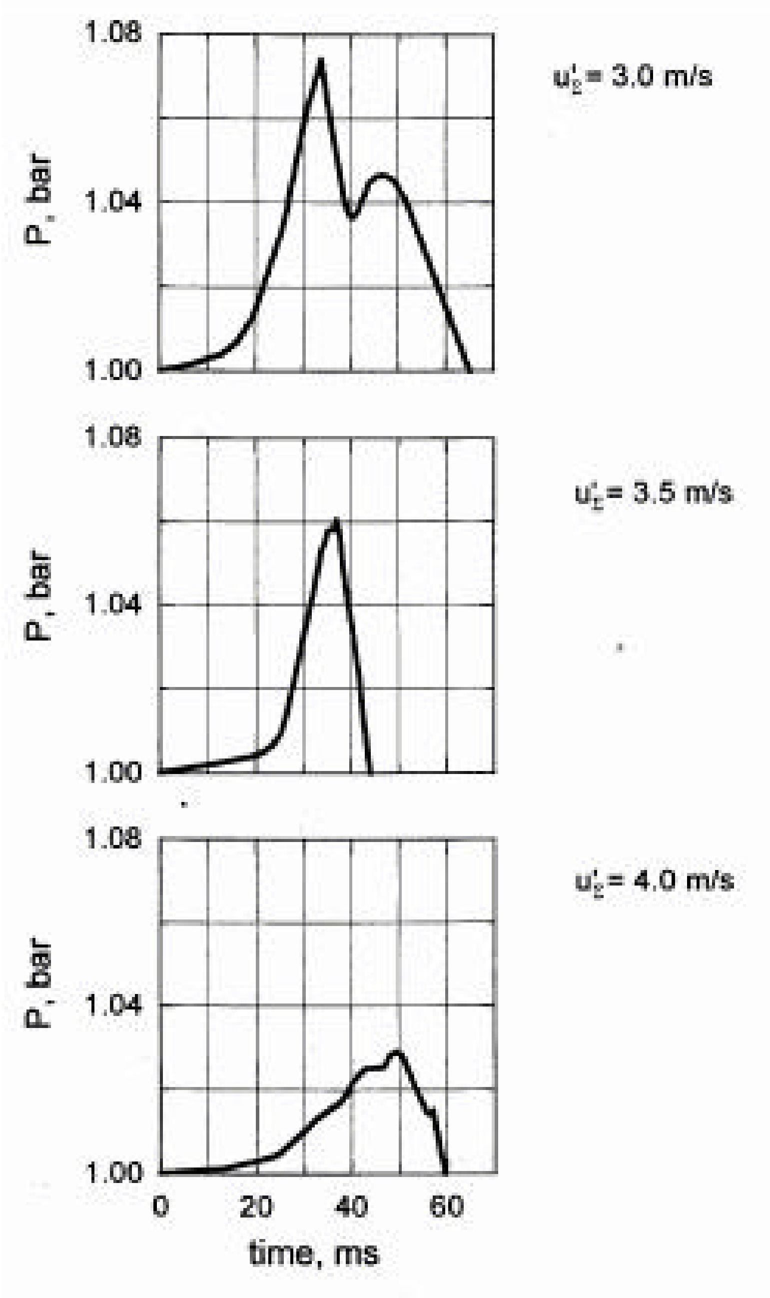

Figure A.1.9. Pressure-time curves at an extinction limit for turbulent flames in hydrogen-air-steam mixtures ($\phi$ = 0.2; 10% $H_2O$; $P_0$=1 bar; $T_0$=398K).

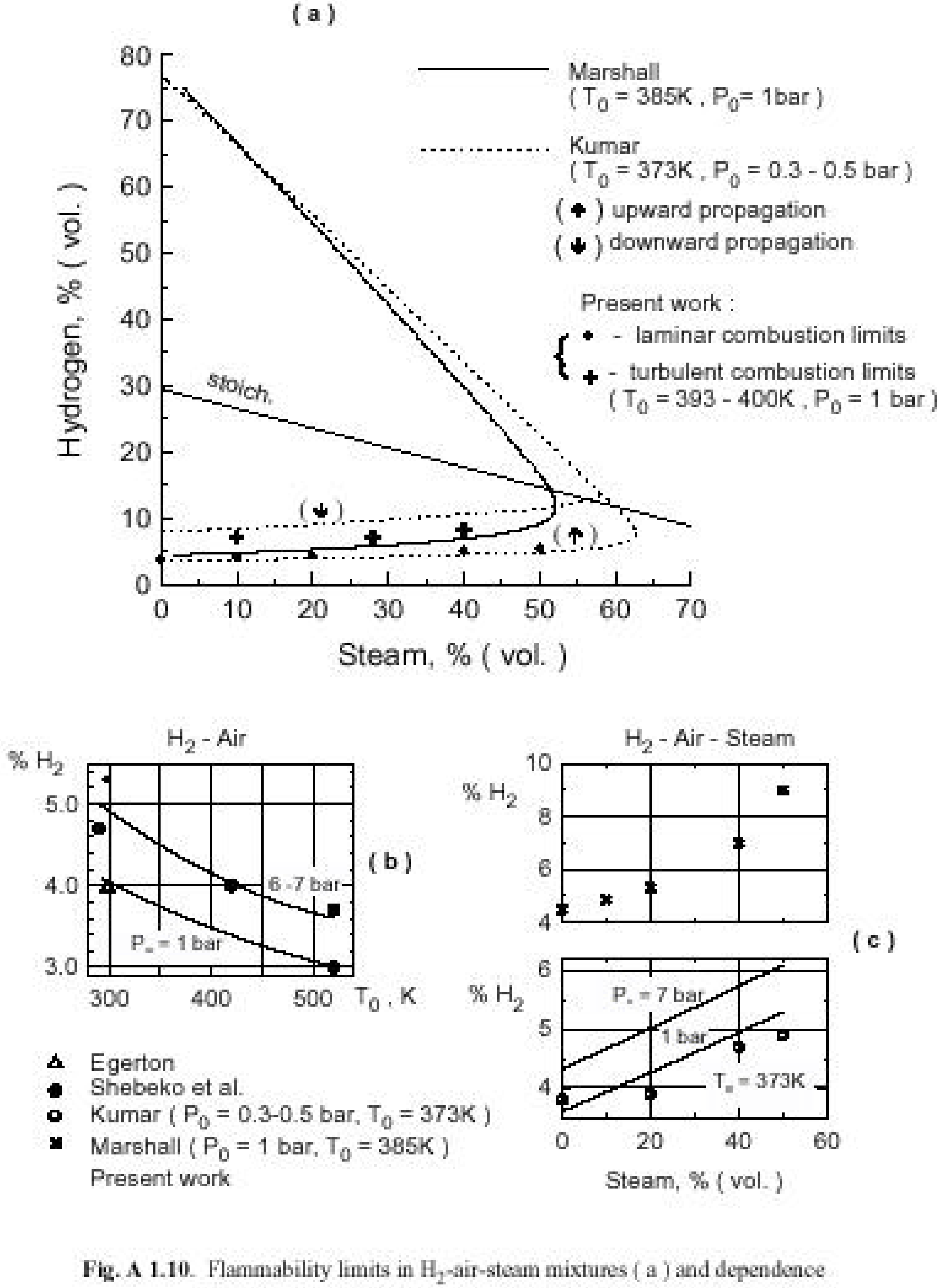

**Fig. A 1.10.** Flammability limits in $H_2$-air-steam mixtures ( a ) and dependence of limit hydrogen concentration on initial pressure and temperature in the lean $H_2$-air ( b ) and $H_2$-air-steam mixtures ( c ).

**Figure A.1.5-1 Flammability limits in $H_2$-air-steam mixtures (a) and dependence of limit hydrogen concentration on initial pressure and temperature in the lean $H_2$-air (b) and $H_2$-air-steam mixutes (c).**